Delayed Output Feedback Control for Gait Assistance With a Robotic Hip Exoskeleton

Bokman Lim, Jusuk Lee, Junwon Jang, Kyungrock Kim, Young Jin Park, Keehong Seo, and Youngbo Shim

***Abstract*—In this paper, we propose a new and simple control strategy for gait assistance with a hip exoskeleton robot. This controller is based on the time delayed, self-feedback known for stabilizing oscillatory systems under certain conditions. In this controller, there are no separate estimators for the gait phase nor the environment, yet the controller can be generalized to operate under various walking conditions (e.g., stair and ramp walking). We first define a state variable representing the current leg's movement with hip joint angles. A simple assistance control can be described in closed-loop form with the delayed state feedback. By assigning the appropriate time-delay and self-feedback gain, we can generate assistive torques stably under the interaction between human and exoskeleton. The controller provides immediate and smooth assistance to user movement by reflecting the change of leg motion at every control period. The proposed joint-angle-based delayed-feedback assistance controller can operate under various walking speeds and environmental changes (e.g., stairs and ramps) without the need for additional sensors, computational processing, and parameter adjustment. Using a simple leg swing model, we perform a stability analysis under a simplified condition to provide insights into the effects of the time-delayed feedback in oscillatory systems. Then, we experimentally validate the efficacy of the proposed assistance controller by measuring the metabolic energy expenditure for level treadmill walking. We also test and analyze the generated assistive torques and power under the different walking conditions to show the generalizability of the controller.**

***Index Terms*—Exoskeleton robot control, hip assistance, rehabilitation robotics, time-delayed feedback.**

I. Introduction

Wearable exoskeletons have attracted attention in the field of elderly care because many countries are facing a rapid increase in elderly population. Actuated exoskeletons can assist the elderly to give them a more independent lifestyle. The device should operate in real-world settings, such as in the users' homes and outdoors, to maximize gait training and assistance from the device. Some of the challenges are that the device must be lightweight with self-contained power source, and should be easy to wear without any assistance from others.

Another challenge is designing a stable and robust controller with limited sensors that can operate in a complex environment (e.g., obstacles, ramps, and stairs). Reducing the number of sensors that require calibration or additional mounting is desirable for usability and ease of device maintenance. Furthermore, the controller should provide safe assistance to those with irregular noncyclic walking patterns, such as patients with severe stroke, charcot–marie–tooth, and Parkinson's disease.

Manuscript received November 4, 2018; accepted April 19, 2019. Date of publication May 16, 2019; date of current version August 1, 2019. This paper was recommended for publication by Associate Editor R. D. Gregg and Editor E. Yoshida upon evaluation of the reviewers' comments. *(Corresponding author: Bokman Lim.)*

The authors are with the Samsung Advanced Institute of Technology, Suwon 16678, South Korea (e-mail: bokman.lim@samsung.com; jusuk7.lee@samsung.com; jw526.jang@samsung.com; kyungroc.kim@samsung.com; yaja.park@samsung.com; keehong.seo@samsung.com; ddalbo.shim@samsung.com).

Color versions of one or more of the figures in this paper are available online at http://ieeexplore.ieee.org.

Digital Object Identifier 10.1109/TRO.2019.2913318

Existing hip assistance algorithms are mainly divided into two groups according to gait phase estimation methods: oscillator-based method and finite state machine (FSM) based method. In oscillator-based methods [1]–[5], the gait cycle (0–100%) is continuously estimated by adaptive oscillators. In the FSM-based methods [6]–[8], gait events, such as foot-strike/toe-off (or stance/swing phase), are discretely detected by FSM transition rules. Although the two groups have distinctive features in gait recognition, they follow common feedforward-based control rules: 1) first estimate gait phase and parameters (e.g., speed, timing of leg swing) from user's prior steps; and 2) then generate assistive torques.

These approaches work well in cyclic walking condition or in uniform environments. However, they do not work well in irregular gait patterns involving the sudden stop in the middle of the swing or changing the direction of the swing (e.g., backward walking) because the existing methods improve the performance of the gait estimator (accuracy and speed) by assuming the gait periodicity. The use of large assistive torques is particularly problematic because the residual motion created by the device can be registered as user motion thus creating an unstable oscillation. This poses safety problems to those with poor balance.

Nagarajan *et al.* [9] suggested an admittance control strategy based on modifying the dynamic response of the coupled human–exoskeleton system to overcome the disadvantages of depending on the periodicity of the gait motion. The feedback controller is capable of achieving the desired response while guaranteeing coupled stability. Martelli *et al.* [10] showed that some control strategies can still be transparent with zero-torque mode even during balance recovery conditions (nonsteady walking patterns). Moreover, Parri *et al.* [11] demonstrated control strategies to cope with several out-of-lab scenarios. Nevertheless, reliably coping with irregular gait patterns, such as those observed in patients or elderly with gait abnormalities, is still challenging.

We present a novel control strategy for gait assistance to address many of the challenges described above. The assistance method is based on the time-delayed, self-feedback control [12] known for stabilizing oscillatory systems under certain conditions [13], [14]. Delays are inherent in human–exoskeleton interactive control. Adding the controlled time delay in the self-feedback control loop, we can generate assistive torques stably under the interaction between human and exoskeleton. A simple assistance control can be described in a closed-loop form with the delayed state feedback. The proposed delayed feedback assistance controller can operate in various gait speeds and environmental changes (e.g., stair, ramp up/down) with only hip angular sensors without the need for gait phase and environment recognizers. Even in irregular ground conditions, such as stairs, sudden stopping and forward/backward walking directions can be appropriately handled. Delay factors are generally known to negatively affect system stabilization [15]. Hence, most of the predictive controllers are solved through delay compensation using additional sensing or estimation [2], [16]. On the other hand, while limited, there are applications of time-delayed feedback control in mechanical systems that utilize the time delay (e.g., damping control in vibrating machining tools [17], [18]). Chopra *et al.* [19] proposed the master/slave synchronization algorithm with constant time delay. Moon [20] also suggested the self-synchronization control

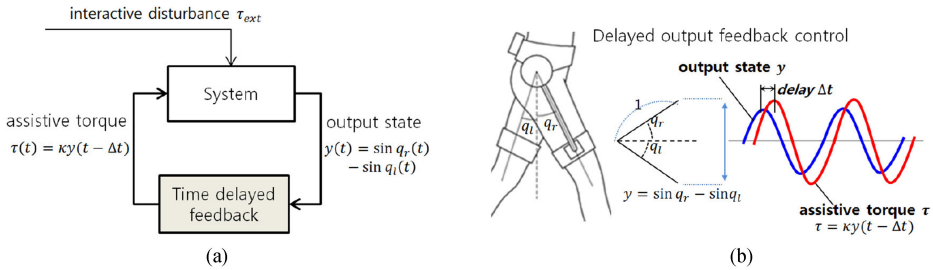

Fig. 1. Gait assistance strategy with DOFC. q_r and q_l are the right and left hip angles, respectively. κ is the feedback gain. (a) Self-feedback control loop. (b) Assistance strategy.

method with time delay to control the swing phase of the compass-gait biped. To the best of our knowledge, this is the first time a time-delayed feedback control is used in a human gait assistance robot.

There are two ways to add delays to the system: 1) phase lag (delay in phase domain) and 2) time delay (delay in time domain). Even though a similarity can be found between the two methods, note that a difference can be observed in actual applications. Unlike the time-delay approach, the phase lag strategy requires a process to estimate the current gait phase. Therefore, the effectiveness of the assistive strategy depends on the performance of the gait phase estimator/predictor. In most cases, additional strategies are needed to achieve stable assistance control even in irregular movements. In the case of Honda's stride management system [1], which uses a strategy to maintain the phase difference between the wearer's walking rhythm and the virtual pacemaker, instead of directly controlling the phase, they chose to control the target walk-ratio (stride/cadence) with small mutual torques [21].

In contrast, the time-delay control strategy uses the intrinsic generalization property of the self-feedback controller [13]. The suggested time delayed, self-feedback controller provides immediate and smooth assistance to user movement by reflecting the change of leg motion at every control period without phase estimation process. Even when the gait periodicity is not guaranteed, a relatively large assistive torque can be stably applied as compared with the existing methods.

This paper is organized as follows. Section II provides an assistance strategy with the time-delayed, self-feedback control scheme with stability analysis under simplified assumptions. Section III provides the experimental results for various walking conditions and Section IV concludes this paper.

II. Assistance Control Strategy

A. Background

Our previous approaches [5], [7], [8] used a method of recognizing the correct gait phase and/or event similar to the existing methods, then generating appropriate torque profile associated to the estimate gait phase/event. These methods were effective in steady walking of healthy persons, but not in patients and elderly people who were more irregular in their walking patterns [22]. Because these individuals are more vulnerable to external perturbations, a slight mismatch between their intended motion and the device assistance can be fatal. Events like this can potentially change the users to walk in a more cautious gait which could defeat the purpose of using this device. To overcome this problem, we propose a simple feedback controller that directly responds to the wearer's hip pattern changes.

Previous studies on biomechanics of human gait showed coupling between joint kinematics and kinetics at various walking speeds [23]. We take the strategy of generating the assistive torque to couple to the hip angle based on this human gait biomechanics. We implemented this strategy in a time-delayed self-feedback control scheme. The time-delayed feedback control itself is known for stabilizing the oscillatory system under some conditions [13], [14]. In addition, we can tune the assist timing by adjusting the constant time-delay value.

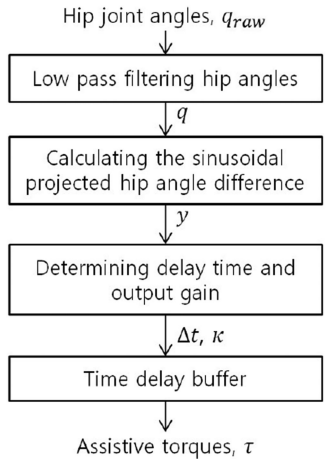

Fig. 2. Control flow for hip assistive torque generation.

B. Delayed Output Feedback Control (DOFC) for Gait Assistance

Fig. 1 shows our gait assistance strategy for the hip exoskeleton. We first define a feedback output state y that represents the projected leg motion

$$y(t) = \sin q_r(t) - \sin q_l(t) \tag{1}$$

$$\tau(t) = \kappa y(t - \Delta t) \tag{2}$$

where q_r and q_l are the right and left hip angles, respectively. We use the sinusoidal projected hip angle difference to normalize the output state from -1 to 1. The assistance torque τ is then generated through a combination of appropriate time delays Δt and control gain κ.

As shown in Fig. 1(a), this simple self-excited feedback control method does not include a gait phase estimator as well as a reference lookups for generating torque profiles. The assistance torque is immediately applied following the movement of the user by reflecting the change of leg motion at every control period ($=0.01$ s). Note that in our system, the assistance algorithm is updated with 100 Hz control frequency. The time delays are approximately 0.15–0.35 s (except the delay from low-pass filtering). Fig. 2 shows the detailed control flow of the suggested method. First, the left and right hip joint angles are sensed from the angular sensors located at the hip joints. The sensed hip angle q_{raw} is smoothed by passing through a first-order low-pass filter (LPF)

$$q^{\text{cur}} = (1 - \alpha)q^{\text{prv}} + \alpha q^{\text{cur}}_{\text{raw}},\ (0 < \alpha < 1) \tag{3}$$

where q^{cur} is the currently smoothed hip angle, q^{prv} is the previously smoothed hip angle, $q^{\text{cur}}_{\text{raw}}$ is the currently sensed original hip angle, α is the smoothing factor. The added delay by the LPF is merely a constant

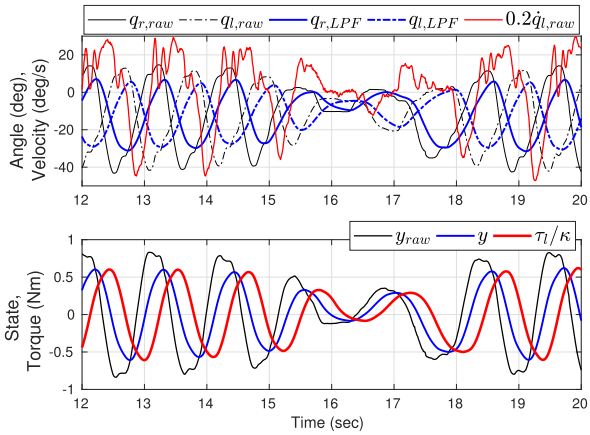

Fig. 3. Relationship between the output state y and the assistive torque divided by gain, τ_l/κ (only the left hip torque is shown for easy understanding). The time delay Δt is 0.25 s. The added delay from the LPF is 0.13 s; hence, the actual total time delay between the state y_{raw} and the assistive torque τ_{left} is 0.38 s. q_{raw} is the original hip joint angle; q_{LPF} is the low-pass filtered hip angle; and $\dot{q}_{l,\text{raw}}$ is the left hip joint velocity. An example control data is obtained with our hip exoskeleton (see Fig. 9).

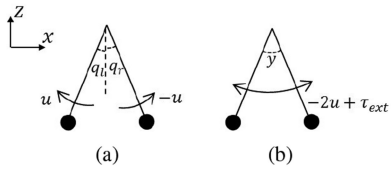

Fig. 4. Simplified pendulum models for leg swing dynamics. (a) original. (b) reduced.

offset value added to the controlled delay Δt. The smoothing factor $\alpha = 0.05$ (cutoff frequency $f_c \approx 0.84$ Hz) in (3) was selected by trial and error to smooth out the output torque. Since the output range of the state increases as the walking speed (or frequency) increases, the attenuation by the filter is compensated to some extent. Normally, when walking speed increases, stride and cadence increases simultaneously [24].

Notice that the added delay from the LPF is approximately 0.13 s (when walking around 4 km/h); thus, the actual total time delays are approximately 0.3–0.5 s. By increasing or decreasing the default time-delay value $\Delta t = 0.25$ s (except the LPF delay) in Fig. 3, we can smoothly adjust the assistance timing. For example, with the maximum swing speed as a reference point (near the intersection of both legs), assistance may come in beforehand (early timing) or may come later (late timing). We can increase or decrease the magnitude of assistive torques by increasing or decreasing the self-feedback gain κ.

C. Stability Analysis With the Simple Swing Leg Model

We analyzed how the adjustment of the assistance parameters (time delay, feedback gain) affects the overall interaction system stability with the simple pendulum models in Fig. 4. Here, we make several simplified assumptions as follows.

1) Human body is represented as two point mass pendular model.
2) Foot-to-ground contact dynamics are omitted.
3) Small angle approximation is used to calculate the y.

The motivation here is to gain insight into how the characteristics of the overall system changes with respect to the parameter changes rather than to find the optimum parameter values of the actual system.

Modeling swing leg dynamics as simple pendulums [Fig. 4(a)], the dynamic equations can be represented in the following form:

$$I\ddot{q}_r(t) + B\dot{q}_r(t) + K\sin q_r(t) = -u(t) \tag{4}$$

$$I\ddot{q}_l(t) + B\dot{q}_l(t) + K\sin q_l(t) = u(t)$$

$$u(t) = \kappa y(t - \Delta t)$$

$$y(t) = \sin q_r(t) - \sin q_l(t) \tag{5}$$

where I ($= I_{\text{leg}}$) is the moment of inertia; K ($= MgL_c$) is the spring-like constant; B is the damping constant; M is mass; L_c is the length between the pivot point and the mass center; g is the gravitational acceleration; κ is the amplifying gain determining torque magnitude; and u is the hip joint input torque.

Introducing the external torque τ_{ext} ($= \tau_{\text{resist}} + \tau_{\text{drive}}$) and assuming that the ground projected hip motion is similar to the joint space hip motion ($\sin q_r - \sin q_l \approx q_r - q_l$), the above equations can be equivalently formulated as the following negative delayed output feedback problem (DOFC) [Fig. 4(b)]:

$$\ddot{y}(t) + b\dot{y}(t) + ky(t) = -2ay(t - \Delta t) + \tau_{\text{ext}}$$

$$y(t) = q_r(t) - q_l(t)$$

$$\tau_{\text{ext}} = \{-k_{\text{ext}}y(t) - b_{\text{ext}}\dot{y}(t)\} + a_{\text{ext}}\cos(wt) \tag{6}$$

where a ($= \kappa/I$) is the amplifying coefficient; k ($= K/I$) is the stiffness coefficient; b ($= B/I$) is the damping coefficient; and τ_{resist} is the resistive torque by the human–exoskeleton interaction (simply modeled with state dependent stiffness and damping resistance). We assume that the resistive interaction force is large when the swinging leg changes direction near the heel contact, where y is large ($q_r - q_l \gg 0$) rather than near the hip intersection ($q_r \approx q_l$) during walking. τ_{drive} is the sinusoidal user-driven torque.

Under free response (i.e., under a motion of the system caused by nonzero initial conditions and a zero excitation $\tau_{\text{drive}} = 0$), (6) can be written in matrix form as follows:

$$\dot{\mathbf{y}}(t) = \mathbf{A}_0\mathbf{y}(t) + \mathbf{A}_1\mathbf{y}(t - \Delta t) \tag{7}$$

where

$$\mathbf{A}_0 = \begin{bmatrix} -b - b_{\text{ext}} & -k - k_{\text{ext}} \\ 1 & 0 \end{bmatrix}$$

$$\mathbf{A}_1 = \begin{bmatrix} 0 & -2a \\ 0 & 0 \end{bmatrix},\ \mathbf{y} = \begin{bmatrix} \dot{y} \\ y \end{bmatrix}.$$

Using the matrix Lambert function $\mathbf{W}$, which is defined by $\mathbf{W}(\mathbf{A})e^{\mathbf{W}(\mathbf{A})} = \mathbf{A}$, the transcendental characteristic equation can be written as follows:

$$s\boldsymbol{I} = \frac{1}{\Delta t}\mathbf{W}(\mathbf{A}_1\Delta t e^{-\mathbf{A}_0\Delta t}) + \mathbf{A}_0 \tag{8}$$

where $\boldsymbol{I}$ is the identity matrix. The stability condition can be obtained by finding the root of the characteristic equation (see [14], [25], [26] for a general discussion of the matrix Lambert function and stability analysis)

$$\det\left\{s\boldsymbol{I} - \left[\frac{1}{\Delta t}\mathbf{W}(\mathbf{A}_1\Delta t e^{-\mathbf{A}_0\Delta t}) + \mathbf{A}_0\right]\right\} = 0. \tag{9}$$

The parameters of the swing dynamic model corresponding to a person with a height of 165 cm and a weight of 55 kg are as follows: $I = I_{\text{leg}} \approx 1$ kgm^2, $K \approx 30$ kgm^2/s^2, $M = 8.86$ kg, $L_c = 0.3483$ m (human parameters are approximated and slightly modified with the simple regression function in the literature [27]. We set the resistive stiffness and damping coefficients as $k_{\text{ext}} = 100$, $b_{\text{ext}} = 0.1$, assuming that small resistive forces occur. As can be seen in the literature [9], the actual coupling stiffness and damping coefficient are much larger. The increase in the stiffness and damping coefficients greatly increased the stable operating area (see Figs. 7 and 8). For the given conditions

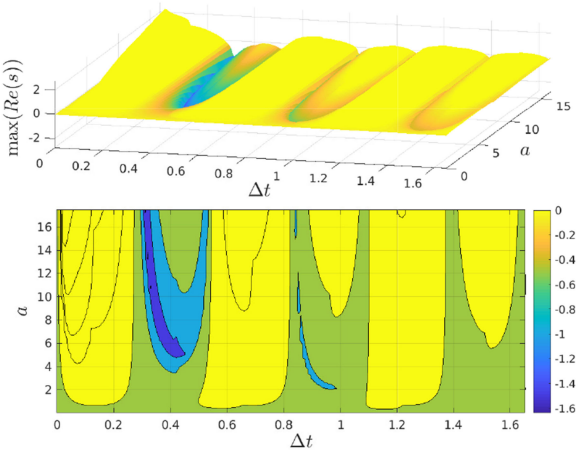

Fig. 5. Largest real part of the roots of the characteristic equation as a function of time delay Δt and gain a. The two-dimensional projection is at the bottom. The nonnegative region (nonyellow) represents the stable control region. The principal branch of the Lambert $\mathbf{W}$ function is solved using the lambertw function in MatlabR2017.

$k = K/I = 30$, $b = B/I = 0.01$, $k_{\text{ext}} = 100$, $b_{\text{ext}} = 0.1$, Fig. 5 shows the stable region (blue area) for the different time delay Δt and control gain a.

With the selected time delay $\Delta t = 0.4$ s, we performed a numerical simulation with the delayed differential equation (DDE) (6). We used the dde23 function in MatlabR2017 as the DDE solver. The initial conditions were set to $\dot{y}(0) = 1$ (nonzero for the initial perturbation), $y(0) = 0$. Fig. 6 shows the free and forced response for the system. For the free response (a representation of stopping from walking), fast convergence only occurred with the time delayed case as in Fig. 6(a). For the forced response (representing a step perturbation), the system stabilized only for the time-delayed case as in Fig. 6(b).

For the fixed $a = 5$ corresponding to the assist intensity, we observed the relation of the largest real value of the roots and the time delay. As the stiffness coefficient $k + k_{\text{ext}}$ increased, the stable region shifted to the lower left as in Fig. 7. As shown in Fig. 8, the graph moved downward, and the stable region increased as the damping coefficient $b + b_{\text{ext}}$ increased. The increased stiffness and damping coefficients indicate an increased resistive interaction force. For the above model, the human–exoskeleton resistive interaction force positively affects the stable operation of the system. As mentioned earlier, this analysis makes several simplifying assumptions; we plan to do more rigorous stability analysis for our future work.

III. Experiment

Fig. 9 shows our latest hip exoskeleton prototype, the gait enhancing and motivating system (GEMS). The total system weight is approximately 2.1 kg, and the maximum output torque is approximately 12 N·m. The basic assistance strategy (see Fig. 1) can be extended for both right/left hip assistive torque generation $\tau_{r,\text{des}}$, $\tau_{l,\text{des}}$ by modifying the original torque $\tau(t) = \kappa(y - \Delta t)$ with the multiple gains.

Right step (right flexion, left extension) assistance

$$\tau_{r,\text{des}}(t) = -\tau(t) \cdot \beta_R \cdot \beta_{\text{Rhip}}$$
$$\tau_{l,\text{des}}(t) = \tau(t) \cdot \beta_R \cdot \delta_R \cdot \beta_{\text{Lhip}} \quad (10)$$

Left step (left flexion, right extension) assistance

$$\tau_{l,\text{des}}(t) = \tau(t) \cdot \beta_L \cdot \beta_{\text{Lhip}}$$
$$\tau_{r,\text{des}}(t) = -\tau(t) \cdot \beta_L \cdot \delta_L \cdot \beta_{\text{Rhip}} \quad (11)$$

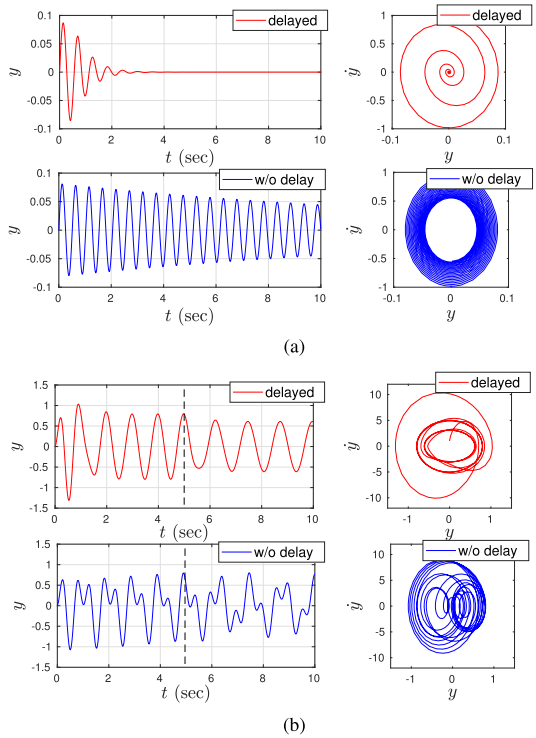

Fig. 6. Free and forced response in time domain (right figure is its phase portrait). The dashed vertical line represents a perturbation by switching the driving frequency from w to $0.8w$ (like changing the walking speed). We set the sinusoidal driving torque, $a_{\text{ext}} = 60 (>> a)$, $w = 2\pi/T, T = 1$ s (representing 1 Hz frequency walking). In delayed cases, we set the time delay Δt as 0.4 s (w/o delay means $\Delta t = 0$). (a) Free response ($\tau_{\text{drive}} = 0$). (b) Forced response ($\tau_{\text{drive}} = a_{\text{ext}} \cos(wt)$).

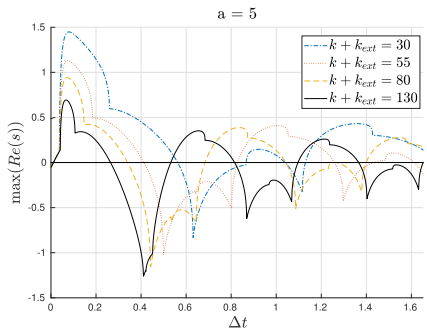

Fig. 7. Largest real part of the roots of the characteristic equation as a function of time delay Δt for the selected stiffness coefficients.

where β_R and β_L are the right and left step assistance gains, respectively; right step assistance denotes right hip flexion and left hip extension assistance; left step assistance denotes left hip flexion and right hip extension assistance; δ_R and δ_L denote the extension/flexion assistance ratios for the right and left step assistance, respectively; and β_{Rhip} and β_{Lhip} denote the right and left hip assistance gains, respectively. Various combinations of asymmetric flexion/extension assistance can be set by adjusting these gains.

We performed several experiments to validate the effectiveness of our DOFC-based assistance. We first evaluated the basic assistance function by comparing the metabolic energy consumption with and without the exoskeleton. We also performed generalizability tests for various speed and environmental changes by comparing the generated torque and power.

TABLE I
EXOSKELETON GENERATED JOINT TORQUE AND POWER, HUMAN REDUCED METABOLIC COST

Subject No.	Assist mode	Cadence (steps/min)	Exo generated joint torque and power				Human reduced metabolic measurement		
			τ_{RMS} (Nm)	τ_{MAX} (Nm)	MPP (W)	MNP (W)	NMR (W/kg)	rNMR (W/kg)	rNMR (%)
1	Exo1	107	5.6	8.0	9.4	-0.14	2.61	0.51	16.3
	Exo2	107	6.5	9.5	11.0	-0.14	2.48	0.64	**20.5**
2	Exo1	105	5.6	8.8	9.6	-0.16	2.64	0.65	19.8
	Exo2	105	6.5	10.7	11.2	-0.16	2.47	0.82	**24.9**
3	Exo1	111	5.5	9.1	10.5	-0.06	2.20	0.52	**19.3**
	Exo2	115	6.4	10.6	12.5	-0.10	2.34	0.39	14.1
4	Exo1	104	5.5	8.7	8.6	-0.09	2.40	0.60	**19.9**
	Exo2	109	6.4	10.8	10.3	-0.07	2.71	0.29	9.5
5	Exo1	113	5.4	8.4	10.0	-0.10	2.56	0.36	12.3
	Exo2	113	6.3	9.7	11.9	-0.10	2.40	0.52	**17.8**
6	Exo1	115	5.5	8.3	11.5	-0.14	2.81	0.56	**16.6**
	Exo2	119	6.2	9.6	12.7	-0.05	2.90	0.47	13.9
Mean (±SD)	Exo1	109±4	5.5±0.1	8.6±0.4	9.9±1.0	-0.11±0.04	2.54±0.21	0.53±0.10	17.4±2.9
	Exo2	111±5	6.4±0.1	10.1±0.6	11.6±0.9	-0.10±0.04	2.55±0.21	0.52±0.19	16.8±5.5
	Best						2.46±0.20	0.61±0.11	**19.8±2.9****

τ_{RMS}: RMS (root mean square) torque; τ_{MAX}: maximum torque; MPP: mean positive power; MNP: mean negative power; NMR: net metabolic rate; rNMR: reduced net metabolic rate from free walking condition (No exo). The bold emphases denote the percent reduction in the best condition of the two assist modes. **p-value$<$ 0.001 for paired t-test (No exo versus Exo best).

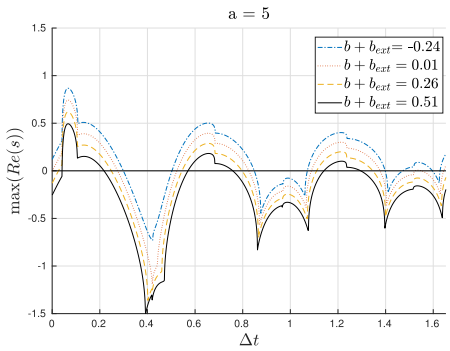

Fig. 8. Largest real part of the roots of the characteristic equation as a function of time delay Δt for the selected damping coefficients.

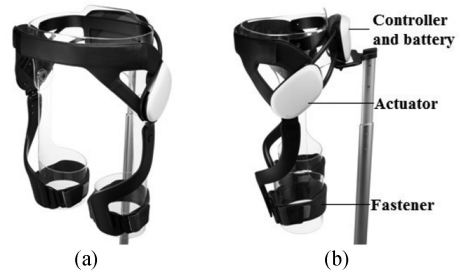

Fig. 9. Hardware prototype for gait assistance, GEMS. Hip joints are actuated to generate assistive forces. (a) Front. (b) Side.

In the rest of this paper, the term "time delay" denotes the Δt without the delay term from the LPF. The time delay caused by the joint angle LPF was approximately 0.13 s (when walking around 4 km/h); hence, the actual total time-delay value was $\Delta t + 0.13$ s.

A. Walking Assistance by Transferring Power From the Exoskeleton to the User

Six male subjects participated in the metabolism experiment (age: 41 ± 3.2; weight: 71 ± 5.0 kg; height: 174 ± 8.2 cm; mean ± standard deviation). All subjects had prior experience walking with the device. The treadmill speed was set to 4 km/h for all subjects. The time-delay Δt value was fixed at 0.2 s; and the same extension/flexion assistive torque ratio was used.

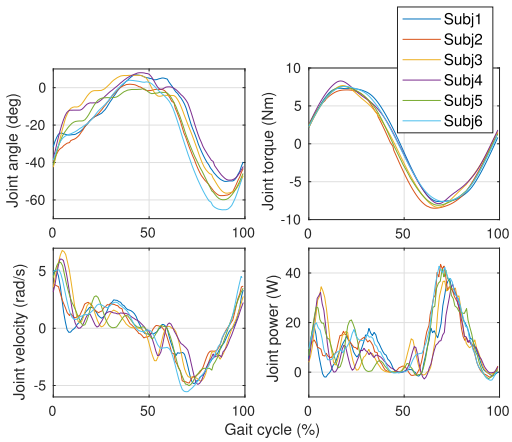

Fig. 10. Exoskeleton hip joint sensing data for six subjects with Exo1 mode. The joint torque represents the generated input assistance torque. The joint power is calculated by multiplying the joint torque by the joint velocity.

First, the subjects stood for 5 min (and again at the end of the experiment) to obtain the average baseline, in which to subtract the walking data to obtain the net metabolic rate. They then walked without the exoskeleton (No exo) for 6 min (and again right before the final 5-min stand) to obtain the average metabolic rate for a normal walking condition. Subsequently, they wore the exoskeleton and walked on the treadmill under two assistance modes (Exo1 and Exo2). The RMS torques for Exo1 and Exo2 modes were approximately 5.5 and 6.5 N·m, respectively. The execution order of the two modes was randomized. We took the median of the last 3 min of each condition to represent the metabolic rate expended at those conditions. The K5 "breath by breath" portable metabolic system (COSMED, Rome, Italy) was used to measure the metabolic energy expenditure. The subjects were required to fast for a minimum of 2 h prior to metabolic testing to reduce bias from food intake.

Table I presents the metabolic measurement result and assistance input data. Fig. 10 shows the joint angle, angular velocity, generated

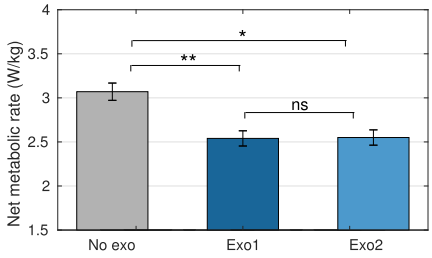

Fig. 11. Net metabolic rate for 4 km/h speed walking on the treadmill. $^{**}p$-value < 0.001, $^{*}p$-value < 0.05, ns: not statistically significant (p-value $= 0.87$).

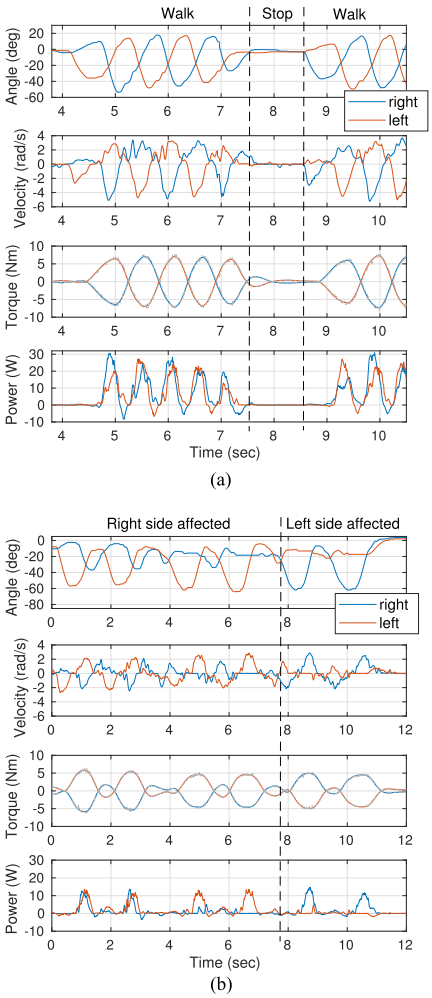

Fig. 12. Hip joint angle, velocity, torque, and power trajectories for the selected irregular gait motions. The hip joint sensing data are obtained from the hip exoskeleton. The walk–stop–walk ($\Delta t = 0.25$ s, $\kappa = 10$) and the asymmetric walk ($\Delta t = 0.25$ s, $\kappa = 8$) are performed with exoskeleton assistance. In the torque plot, the gray dashed line represents the measured torques (from current sensing), while the blue and red solid lines denote the generated desired assistance torques. (a) Walk-stop-walk. (b) Asymmetric walk (changing affected side).

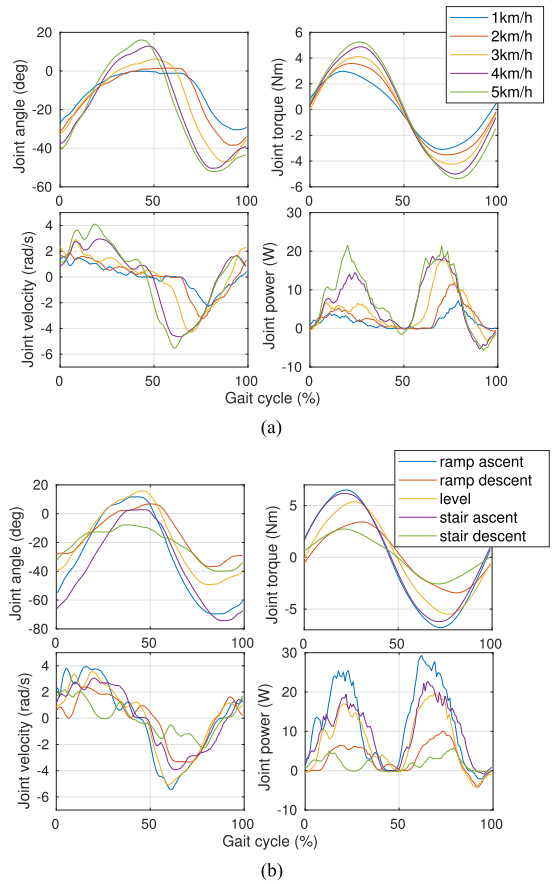

Fig. 13. Exoskeleton hip joint sensing data with the different gait speeds and environments for one subject ($\Delta t = 0.25$ s, $\kappa = 8$). The assistive torque increased as the treadmill speed increased. The assistive torque increased at the stair/ramp ascent, and the assistive torque decreased at the stair/ramp descent. (a) Gait speed changes. (b) Gait environment changes.

Fig. 14. Experimental protocol for walking environment adaptation. The arrow direction of the pass line indicates the order of walking (ramp ascent→ ramp descent→ level→ stair ascent→ stair descent).

torque, and power trajectories on the right hip joint. The data were obtained from the hip exoskeleton. The hip exoskeleton significantly reduced the metabolic cost of walking for all subjects from 16.6 to 24.9%. We used paired t-tests to evaluate the pairwise differences between normal walking without the exoskeleton and assisted walking with the exoskeleton. At the best condition of the two assist modes, the net metabolic cost of walking with the hip exoskeleton (2.46 $\pm$ 0.20 W/kg) was 19.8 $\pm$ 2.9% ($p < 0.001$) reduction compared to the cost of walking without the exoskeleton (3.07 $\pm$ 0.24 W/kg).

The difference between the two assist modes (Exo1 and Exo2) is only the assist strength from having different feedback gain κ ($\kappa_{\text{Exo1}} < \kappa_{\text{Exo2}}$). The desired input RMS torque values for mode Exo1 and mode Exo2 were 5.5 and 6.5 N· m, respectively. It was achieved by adjusting the gain value in advance for each subject ($\kappa_{\text{Exo1}} = 13.2 \sim 16.6$, $\kappa_{\text{Exo2}} = 14.4 - 17.4$). Exo1 mode had a maximum torque value of approximately 8.6 N·m at a relatively low intensity compared to Exo2 mode of approximately 10.6 N· m maximum torque (see Table I). As shown in Fig. 11, no significant difference in the net metabolic rate values between the two modes could be found. A slight increase in cadence caused by the increase in the assistance strength was found, but

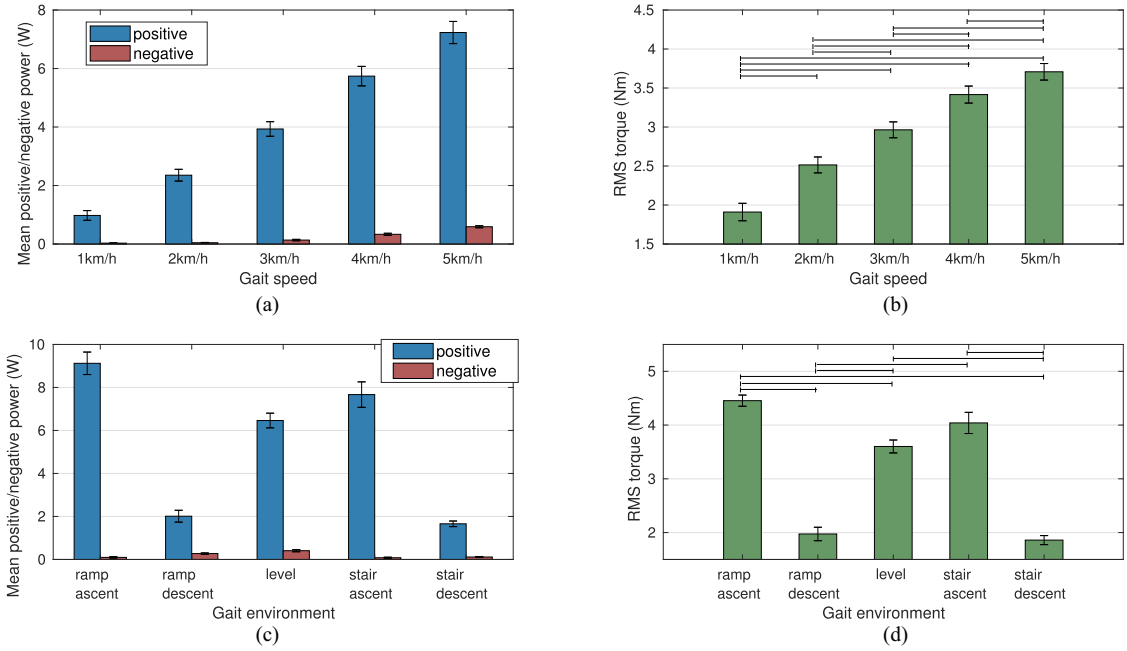

Fig. 15. Assistance adaptation to gait speed and environment changes with the fixed time delay $\Delta t = 0.25$ s and gain $\kappa = 8.0$. Vertical error bars represent the standard error means. Horizontal brackets denote significant differences (p-value < 0.05). (a) Mean power versus walking speed. (b) RMS torque versus walking speed. (c) Mean power versus walking environment. (d) RMS torque versus walking environment.

it was not significant ($p = 0.08$). The net metabolic cost reduction for the Exo1 (2.54 ± 0.21 W/kg) and Exo2 (2.55 ± 0.21 W/kg) modes was $17.4 \pm 2.9\%$ ($p < 0.001$) and $16.8 \pm 5.5\%$ ($p < 0.05$), respectively.

One notable point is that cadence was maintained for subjects 1, 2, and 5, which had a further decrease in metabolic energy in Exo2 (larger assist) mode. This was consistent with our previous findings [28]. On the contrary, subjects 3, 4, and 6, in which the cadence change occurred, did not lead to a greater metabolic energy reduction, even though larger assistive torque and power were delivered. For them, the change of the walking pattern was assumed to be caused by the excessive assistive torque.

B. Application to the Selected Task Transitions

We applied the proposed assistance method to actual task transitions, as shown in Fig. 12. Fig. 12(a) shows the joint angle and assistance torque values during walking task transitions from walk to stop and stop to walk. Fig. 12(b) shows the joint angle and assistance torque values during the asymmetric walking. The asymmetric gait pattern (involving changing the affected side) was generated by step-by-step walking on the stairs. For the walk–stop–walk transition task, the result mean positive and negative power values were 6.1 W and -0.3 W, respectively. For the asymmetric walk, the result mean positive and negative power values were 1.6 W and -0.14 W, respectively. A small negative power value compared to a relatively large positive power supports the idea that the resistive torque generation was minimal. Although not comprehensive, the minimal negative power graph as in Fig. 12 suggests that our controller could appropriately assist in various walking conditions. The assist controller and the output torque is greatly affected by the hip range of motion (ROM) as in Fig. 12(b).

C. Generalization of Assistance Under Various Gait Speeds and Walking Environment

The same six male subjects wore the exoskeleton and walked with assistance. The assistance control parameters were fixed with the same values ($\Delta t = 0.25$ s, $\kappa = 8$) for all subjects as they walking under various gait speeds and walking environment. Through this experiment, we showed how the proposed assistance algorithm can be generalized in assisting in various conditions by showing the torque and power profiles.

An one-way analysis of variance was used to investigate the generalizability of the assistance controller. For the post-hoc analysis, the MATLAB multiple comparison procedure "multcompare" function was used with the comparison type based on Tukeys honestly significant difference criterion. The statistical significance level was set at $\alpha = 0.05$.

1) Gait Speed Changes: The subjects walked on the treadmill under different walking speeds. The treadmill speed increased from 1 to 5 km/h in 1 km/h increment. They walked for 1 min for each speed. We took the last 30 s of each condition to calculate the generated RMS torque and the mean positive/negative power.

Fig. 15(a) and (b) shows the joint torque and positive and negative power. Fig. 15(b) [also in Fig. 13(a)] illustrates how the assistance torque profile changed as the treadmill speed changed all with the same control parameters ($\Delta t = 0.25$ s, $\kappa = 8$). The vertical error bars represent the standard error means, while the horizontal brackets denotes the significant differences ($p < 0.05$). All possible pairs for different speed conditions were significantly different. In the suggested controller, the assistance torques were determined by two factors, namely the control parameters (feedback gain κ, time delay Δt) and the motion state y. Since the control parameters were fixed the individual hip motion, such as the ROM, determines the output torque profile.

2) Gait Environment Changes: Fig. 14 shows the protocol to measure the generated assistive torque and power under different walking environments. The subjects walked with the self-selected speed in different ground conditions (i.e., ramp ascent, ramp descent, level, stair ascent, and stair-descent). We took the section corresponding to each condition to calculate the generated RMS torque and the mean positive/negative power.

Fig. 15(c) and (d) shows the results. As shown in Fig. 13(b), the assistance torque trajectory changed with the gait environment change. Without changing the assistance control parameters ($\Delta t = 0.25$ s, $\kappa = 8$), the generated torque and power values were changed with notable differences. The vertical error bars represent the standard error

means, while the horizontal brackets denote the significant differences ($p < 0.05$). Although some pairs were not significantly different as in Fig 15(d) (ramp ascent versus stair ascent, ramp descent versus stair descent, and level versus stair ascent), the assistive torque values also appropriately changed in accordance with the change of the walking environment.

As shown in Fig. 13(a), the generated assistive torque profile shape has a sine-like wave. Therefore, the RMS torque difference corresponding to each walking condition as in Fig. 15 can represent to some extent the generated profile difference. Biologically, human gait requires higher hip torque and power as the walking speed increases [29]. Stair climbing also requires greater hip torque than downhill [30]. Therefore, generating a larger assistive torque when a larger torque is required may be a desirable characteristic for seamless assistance. Fig. 15(a) and (c) shows positive and negative power during various walking conditions. The large positive power compared to the small negative power indicates that the DOFC controller can operate under various conditions in assisting the user with minimal interference.

IV. Conclusion

In this paper, we presented a novel control strategy for gait assistance. By using the DOFC-based assistance, we can generate assistive torques stably under the interaction between human and exoskeleton. We showed the effectiveness of the assistance method by measuring the metabolic energy expenditure. The proposed algorithm was simple, but powerful because of its generalizability to the user's walking pattern changes. We also showed how the assistance method changes the assistive torques according to the gait pattern change without changing the control parameters.

In the future, we plan to measure the metabolic cost reduction under various walking speeds, slopes, and stairs. In addition, to find the best set of parameters for each individual, we plan to use on-line parameter optimization techniques. It remains to be seen if the single set of optimum parameter values outweigh the cost of introducing an environment recognizer with different set of optimal parameters for each walking condition. Furthermore, we will investigate extending the DOFC assistance method to other exoskeleton types, such as the knee and ankle exoskeletons each with its own state values.

References

[1] K. Yasuhara, K. Shimada, T. Koyama, T. Ido, K. Kikuchi, and Y. Endo, "Walking assist device with stride management system," *Honda R&D Tech. Rev.*, vol. 21, no. 2, pp. 54–62, 2009.

[2] R. Ronsse *et al.*, "Oscillator-based walking assistance: A model-free approach," in *Proc. IEEE Int. Conf. Rehabil. Robot.*, 2011, pp. 1–6.

[3] X. Zhang and M. Hashimoto, "Inhibitory connections between neural oscillators for a robotic suit," in *Proc. IEEE Int. Conf. Robot. Autom.*, 2011, pp. 4182–4187.

[4] T. G. Sugar *et al.*, "Limit cycles to enhance human performance based on phase oscillators," *J. Mech. Robot.*, vol. 7, no. 1, 2015, Art. no. 011001.

[5] K. Seo, S. Hyung, B. Choi, Y. Lee, and Y. Shim, "A new adaptive frequency oscillator for gait assistance," in *Proc. IEEE Int. Conf. Rob. Autom.*, 2015, pp. 5565–5571.

[6] C. J. Walsh, K. Pasch, and H. Herr, "An autonomous, underactuated exoskeleton for load-carrying augmentation," in *Proc. IEEE/RSJ Int. Conf. Intell. Robots Syst.*, 2006, pp. 1410–1415.

[7] B. Lim, K. Kim, J. Lee, J. Jang, and Y. Shim, "An event-driven control to achieve adaptive walking assist with gait primitives," in *Proc. IEEE/RSJ Int. Conf. Intell. Robots Syst.*, 2015, pp. 5870–5875.

[8] J. Jang, K. Kim, J. Lee, B. Lim, and Y. Shim, "Online gait task recognition algorithm for hip exoskeleton," in *Proc. IEEE/RSJ Int. Conf. Intell. Robots Syst.*, 2015, pp. 5327–5332.

[9] U. Nagarajan, G. Aguirre-Ollinger, and A. Goswami, "Integral admittance shaping: A unified framework for active exoskeleton control," *Robot. Auton. Syst.*, vol. 75, pp. 310–324, 2016.

[10] D. Martelli *et al.*, "The effects on biomechanics of walking and balance recovery in a novel pelvis exoskeleton during zero-torque control," *Robotica*, vol. 32, no. 8, pp. 1317–1330, 2014.

[11] A. Parri *et al.*, "Real-time hybrid locomotion mode recognition for lower limb wearable robots," *IEEE/ASME Trans. Mechatronics*, vol. 22, no. 6, pp. 2480–2491, Dec. 2017.

[12] K. Pyragas, "Continuous control of chaos by self-controlling feedback," *Phys. Lett. A*, vol. 170, no. 6, pp. 421–428, 1992.

[13] C. Abdallah, P. Dorato, J. Benites-Read, and R. Byrne, "Delayed positive feedback can stabilize oscillatory systems," in *Proc. IEEE Conf. Amer. Control*, 1993, pp. 3106–3107.

[14] P. Hövel and E. Schöll, "Control of unstable steady states by time-delayed feedback methods," *Phys. Rev. E*, vol. 72, no. 4, 2005, Art. no. 046203.

[15] A. Olbrot, "A sufficiently large time delay in feedback loop must destroy exponential stability of any decay rate," *IEEE Trans. Autom. Control*, vol. AC-29, no. 4, pp. 367–368, Apr. 1984.

[16] T. Takenaka, T. Ishikawa, and K. Yasuhara, "Walking assist device," U.S. Patent Application No. 15/155,603, 2016.

[17] R. D. Robinett, B. J. Petterson, and J. C. Fahrenholtz, "Lag-stabilized force feedback damping," *J. Intell. Robot. Syst.*, vol. 21, no. 3, pp. 277–285, 1998.

[18] S. G. Chen, A. G. Ulsoy, and Y. Koren, "Computational stability analysis of chatter in turning," *J. Manuf. Sci. Eng.*, vol. 119, no. 4A, pp. 457–460, 1997.

[19] N. Chopra, M. W. Spong, and R. Lozano, "Synchronization of bilateral teleoperators with time delay," *Automatica*, vol. 44, no. 8, pp. 2142–2148, 2008.

[20] J. S. Moon, "Stability analysis and control for bipedal locomotion using energy methods," Ph.D. dissertation, Univ. Illinois at Urbana-Champaign, Champaign, IL, USA, 2011.

[21] K. Yasuhara and Y. Endo, "Walking motion assist device," U.S. Patent 9, 610, 209, 2017.

[22] B. Lim, S. H. Hwang, S. Hyung, J. Lee, Y. Shim, and B. O. Choi, "Ankle pathologic gait assistance of a hip exoskeleton: Simulation and experiment," *IEEE Robot. Autom. Lett.*, vol. 3, no. 3, pp. 2190–2197, Jul. 2018.

[23] C. Frigo, P. Crenna, and L. M. Jensen, "Moment–angle relationship at lower limb joints during human walking at different velocities," *J. Electromyogr. Kinesiol.*, vol. 6, no. 3, pp. 177–190, 1996.

[24] R. Tanawongsuwan and A. Bobick, "A study of human gaits across different speeds," Georgia Tech, Atlanta, GA, Tech. Rep., 2003.

[25] F. M. Asl and A. G. Ulsoy, "Analysis of a system of linear delay differential equations," *J. Dyn. Syst. Meas. Control*, vol. 125, no. 2, pp. 215–223, 2003.

[26] S. Yi, P. Nelson, and A. Ulsoy, "Delay differential equations via the matrix Lambert W function and bifurcation analysis: Application to machine tool chatter," *Math. Biosci. Eng.*, vol. 4, no. 2, pp. 355–368, 2007.

[27] D. A. Winter, *Biomechanics and Motor Control of Human Movement*. Hoboken, NJ, USA: Wiley, 2009.

[28] J. Lee, K. Seo, B. Lim, J. Jang, K. Kim, and H. Choi, "Effects of assistance timing on metabolic cost, assistance power, and gait parameters for a hip-type exoskeleton," in *Proc. IEEE Int. Conf. Rehabil. Robot.*, 2017, pp. 498–504.

[29] M. Grimmer, "Powered lower limb prostheses," Ph.D. dissertation, Technische Universität Darmstadt, Darmstadt, Germany, 2015.

[30] A. Protopapadaki, W. I. Drechsler, M. C. Cramp, F. J. Coutts, and O. M. Scott, "Hip, knee, ankle kinematics and kinetics during stair ascent and descent in healthy young individuals," *Clin. Biomech.*, vol. 22, no. 2, pp. 203–210, 2007.